ARTICLE

Structural and Magnetic Properties of Chemically Synthesized Pd-Modified $NiFe_2O_4$ Nanoparticles

Shahid Atiq[a*], Shahid M. Ramay[b], Asif Mahmood[c], Saira Riaz[a], Shahzad Naseem[a]

a. Centre of Excellence in Solid State Physics, University of the Punjab, Quaid-e-Azam Campus, Lahore-54590, Pakistan

b. Physics and Astronomy Department, College of Science, King Saud University, P. O. Box 2455, Riyadh 11451, Saudi Arabia

c. Chemical Engineering Department, College of Engineering, King Saud University, P. O. Box 800, Riyadh 11421, Saudi Arabia

(Dated: Received on July 21, 2015; Accepted on November 7, 2015)

Magnetic nanoparticles of $NiFe_2O_4$-Pd composites have been synthesized using a simple, low cost, sol-gel auto-combustion method. As-prepared samples were sintered at 800 °C for 6 h in order to develop the crystalline phase. X-ray diffraction confirmed the spinel structure of the ferrite samples. Structural morphology and size of the nanoparticles were evaluated using a field emission scanning electron microscope. Magnetic hysteresis loops were obtained at 300 and 100 K using a physical properties measurement system. The value of saturation magnetization was observed to decrease at the temperatures with the increase of Pd contents up to 5% but then a sudden rise in saturation magnetization was observed for the addition of 10% Pd in $NiFe_2O_4$.

Key words: Magnetic nanoparticles, Sol-gel auto-combustion, Low temperature magnetic property

I. INTRODUCTION

Extensive use of magnetic nanoparticles (MNPs) in recent years in almost every sphere of daily life motivates the researchers to explore the field systematically for human benefit [1]. In particular, physical and chemical properties of spinel ferrites (MFe_2O_4, M=divalent metal ion) are immensely tailored at nanoscale and thus vastly investigated, mainly due to surface and quantum size effect [2]. Divalent metal (M^{2+}) may reside at two distint sites within spinel structure namely A (tetrahedral) and B (octahedral) sites, leading to normal spinel structure of the type $[M^{2+}]_A[Fe^{3+}Fe^{3+}]_BO_4$ and inverse spinel structure with general formula $[Fe^{3+}]_A[M^{2+}Fe^{3+}]_BO_4$ [3].

The nature and distribution of charges at these sites, in turn decide the electrical and magnetic characteristics of these ferrites. Among these, nickel ferrite ($NiFe_2O_4$) has been widely investigated due to its unique magnetic properties, depending upon particle dimensions, including superparamagnetism [4], high saturation magnetization, and high magnetocrystalline anisotropy [5]. $NiFe_2O_4$ exhibits an inverse spinel structure, Ni^{2+} ions reside at octahedral sites and Fe^{3+} ions are equally distributed between tetrahedral and residual octahedral sites [6]. Owing to this unique structure, application domain of these ferrites can be expanded to many fields, such as ferrofluids, radar absorbing coatings, biochemical devices, sensors and catalytic applications by changing the divalent cation type at octahedral and/or tetrahedral sites [7].

For instance, substitution of Cr at octahedral site in $NiFe_2O_4$ nanopowders has been reported to decrease the coercivity making the resultant compound applicable in high frequency transformer applications [8]. On the other hand, mesoporous $NiFe_2O_4$ has been found as an efficient adsorbent for the removal of Cr(VI) pollutant caused by various industries such as mining, leather tanning, steel making, and pigments [9]. Nanostructured $NiFe_2O_4$ have also emerged as an effective oxidizing and reducing agent when doped with ions like Pd, Au, Pt *etc.* [10]. In particular, $NiFe_2O_4$-Pd magnetically recyclable composites have been recently reported as highly effective catalysts for reduction reactions in liquid phase [11]. The catalytic activity is a surface phenomenon which proceeds by adsorbing the gases from atmosphere, leading to altering the electrical properties of these semiconducting spinel oxides.

In this work, we propose a cast effective synthesis of $NiFe_2O_4$/Pd composites via sol-gel auto-combustion route in order to investigate the effect of Pd (0%−10%) contents in $NiFe_2O_4$ on the structural, morphological, room temperature (RT) and low temperature (LT) magnetic properties. Traditionally, $NiFe_2O_4$ based materi-

*Author to whom correspondence should be addressed. E-mail: shahidatiqpasrur@yahoo.com

al shave been synthesized by variety of methods, *i.e.* solid state reaction method [12], co-precipitation [4, 10], sol-gel [13, 14] and combustion assisted techniques [1, 3]. However, sol-gel based auto-combustion route has emerged as an efficient way to prepare ferrite nanoparticles in a quick time, with high purity and consuming low energy.

II. EXPERIMENTS

Stoichiometric amounts of analytical grade reagents, nickel nitrate ($Ni(NO_3)_2{\cdot}6H_2O$, Alfa Aesar), iron nitrate ($Fe(NO_3)_3{\cdot}9H_2O$, Alfa Aesar), palladium(II) acetate ($C_{12}H_{18}O_{12}Pd_3$, Alfa Aesar) were first dissolved in deionized water separately and then mixed together to make 100 mL solution. Citric acid was used as a chelating agent keeping metal nitrate to citric acid ratio of 1:2. The solution was stirred magnetically on a hot plate at 90 °C for 3 h, leading to a gel formation. At the instance, the temperature of the hot plate was increased to 350 °C. After a few moments, the gel burnt exothermically. The end product was a loose and fluffy powder. The obtained powder samples were sintered at 800 °C for 6 h to develop the crystalline phase. The pellets were formed using an Apex hydraulic press. Crystal structure was investigated by Bruker D-8 Discover X-ray diffractometer (XRD). Structural morphology was determined using Jeol JSM-7600F field emission scanning electron microscope (FESEM). Physical properties measurement system (PPMS, Quantum Design) was employed to explore the magnetic properties.

III. RESULTS AND DISCUSSION

Figure 1 shows the XRD patterns of the samples prepared. To determine the crystal structure, indexing of the diffraction patterns was performed by following the complete procedure as laid by Cullity [15]. Lattice constant was determined using the relation,

$$a = d_{hkl}\sqrt{h^2 + k^2 + l^2} \tag{1}$$

where d_{hkl} is the interplanar spacing between the planes with Miller's indices hkl. Hence, the crystal structure of all the samples was confirmed as spinel cubic with space group Fd3m. It is also evident that addition of Pd contents upto 5% can easily withstand the cubic spinel structure of the host material as no marked difference or any shift in the peak positions is observed. However, the intensity of some peaks in the sample with 10% Pd was decreased along with the complete disappearance of the (422) peak. The lattice constant of pure $NiFe_2O_4$ sample came out to be 8.3390 Å while a minute decrease in lattice constant was observed with the addition of Pd contents upto 10%, as shown in Table I. The patterns were also matched perfectly characteristic

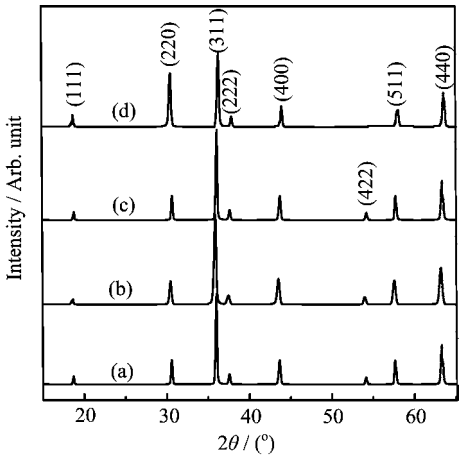

FIG. 1 XRD patterns of (a) $NiFe_2O_4$, (b) 2.5%Pd/$NiFe_2O_4$, (c) 5.0%Pd/$NiFe_2O_4$, and (d) 10%Pd/$NiFe_2O_4$.

TABLE I Calculated values of lattice constant a, unit cell volume V, crystallite size D, bulk density ρ_b (in g/cm^3), X-ray density ρ_x (in g/cm^3) and porosity P of all the samples in the series.

Pd	a/Å	V/nm^3	D/nm	ρ_b	ρ_x	P/%
0%	8.3390	579.885	96.03	5.69	6.45	11.78
2.5%	8.3374	579.551	71.74	5.57	6.58	15.34
5.0%	8.3365	579.364	46.08	5.50	6.69	17.78
10.0%	8.3348	579.009	34.14	5.41	6.81	20.56

reference pattern of $NiFe_2O_4$ (ICSD card 00-010-0325).

The crystallite size, as determined by using Scherrer's formula ($D{=}k\lambda/B\cos\theta$, where k is a constant, λ is wavelength of X-rays, B is full width at half maximum in radians, and θ is the Bragg's angle), was gradually decreased from 96 nm to 34 nm in the series of samples, conferring that Pd contents had a pronounced effect on the crystallite size of ferrite samples. In addition, unit cell volume ($V{=}a^3$), bulk density ($\rho_b{=}m/\pi r^2 h$, where m is mass, r is radius and h is the thickness of the pellet), X-ray density ($\rho_x{=}2M/N_A V$, where M is molecular mass, N_A is the avogadro's no and V is the unit cell volume.) and porosity ($P{=}1{-}\rho_b/\rho_x$) were also affected by Pd concentration, as shown in Table I.

Figure 2 reveals the structural morphology of the samples. Highly smooth and uniform surface of the sample exhibiting grains with sharp and well defined boundaries was observed for the pure $NiFe_2O_4$ sample, as shown in Fig.2(a). The grain sizes were estimated in the 100−120 nm range. As the Pd was added in the pure sample, the grains become more spherical in shape with the reduced sizes. The average grain sizes were in the range of 70, 50, and 40 nm in the samples with 2.5%, 5.0%, and 10% Pd contents. The values of grain sizes were well consistent with crystallite sizes as determined from the diffraction data. A close observation of the

DOI:10.1063/1674-0068/29/cjcp1507158

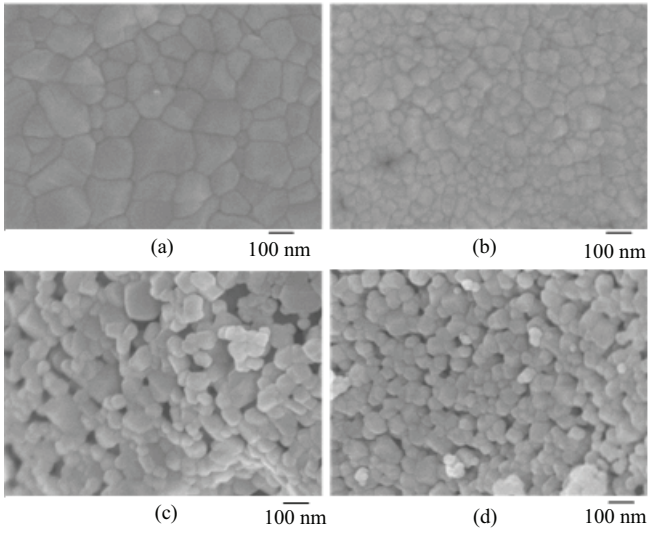

FIG. 2 SEM images of (a) $NiFe_2O_4$, (b) 2.5%Pd/$NiFe_2O_4$, (c) 5.0%Pd/$NiFe_2O_4$, and (d) 10%Pd/$NiFe_2O_4$.

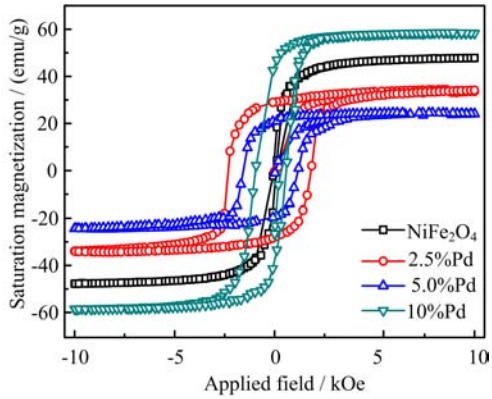

FIG. 3 Magnetic hysteresis loops of $NiFe_2O_4$, 2.5%Pd/$NiFe_2O_4$, 5.0%Pd/$NiFe_2O_4$, and 10%Pd/$NiFe_2O_4$ at 300 K.

SEM images also reveals that the porosity tends to increase (as established earlier from the diffraction data) with the Pd contents making the samples more efficient for catalytic applications.

Figure 3 shows the magnetic hysteresis (M-H) loops of the samples obtained at 300 K, with an applied magnetic field of 10 kOe. The saturation magnetization (M_s) and coercivity (H_c) for the pure $NiFe_2O_4$ sample were found as 47.83 emu/g and 65 Oe, in good agreement with the previous reports [1, 5]. A gradual decrease in M_s was observed for the 2.5%Pd/$NiFe_2O_4$ and 5.0%Pd/$NiFe_2O_4$ sample but a sudden rise in M_s to a value of 58.58 emu/g was witnessed for 10%Pd/$NiFe_2O_4$, as shown in Fig.4. However, the value of H_c showed a variable trend in the series. This decrease in M_s could be attributed to the particles size effect [16].

Low temperature magnetic characteristics of the samples have also been discussed upto 20 K. Here we present M-H loops of the samples obtained at 100 K as shown in Fig.5. At this temperature, the M_s value for the pure $NiFe_2O_4$ sample came out to be 51.67 emu/g, however, a gradual decrease in M_s was observed which came out to be 37.2 and 28.27 emu/g for 2.5%Pd/$NiFe_2O_4$ and 5.0%Pd/$NiFe_2O_4$ samples, respectively. Afterwards, a sharp increase in M_s to a value of 63.24 emu/g was noted for 10%Pd/$NiFe_2O_4$ (Fig.4). The corresponding larger values of M_s at 100 K as compared to that of 300 K could be well attributed to the Weiss theory of ferromagnetism [17]. These magnetic parameters and particle sizes of Pd/$NiFe_2O_4$ are well suited for utilization as effective catalysts for reduction reactions which could also be separated magnetically easily for multiple uses [11].

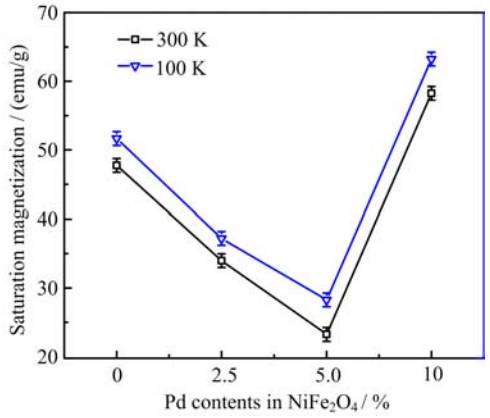

FIG. 4 Dependence of saturation magnetization on Pd contents in $NiFe_2O_4$ at 300 and 100 K.

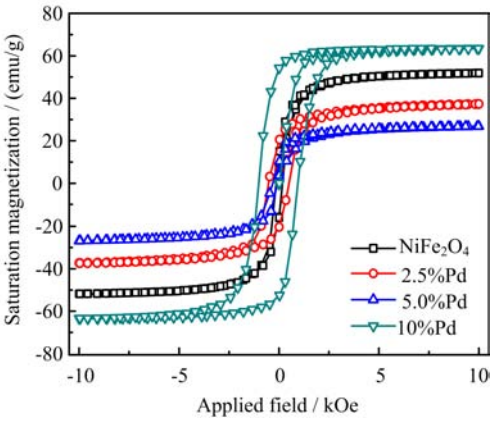

FIG. 5 Magnetic hysteresis loops of $NiFe_2O_4$, 2.5%Pd/$NiFe_2O_4$, 5.0%Pd/$NiFe_2O_4$, and 10%Pd/$NiFe_2O_4$ at 100 K.

IV. CONCLUSION

Sol-gel auto-combustion technique has been successfully employed to synthesize 0−10%Pd/$NiFe_2O_4$

DOI:10.1063/1674-0068/29/cjcp1507158

nanoparticles. X-ray diffraction confirmed the spinel cubic structure of all the samples. Crystallite size was decreased from 96 nm to 34 nm while bulk density was decreased from 5.69 g/cm^3 to 6.41 g/cm^3. X-ray density and porosity were increased from 6.45 g/cm^3 to 6.81 g/cm^3 and 11.78% to 20.56%, respectively. The grains sizes as determined from the SEM images were well consistent with the crystallite sizes evaluated using the diffraction data. The M_s values for $NiFe_2O_4$ were found as 47.83 and 51.67 emu/g at 300 and 100 K, respectively which were gradually decreased to 23.24 and 28.27 emu/g, respectively for 5.0%Pd/$NiFe_2O_4$. A sudden rise in M_s for 10.0%Pd/$NiFe_2O_4$ was witnessed at both the temperatures. The magnetic characteristics of these nano-sized Pd/$NiFe_2O_4$ particles show to be useful as recycle-able catalysts for reduction reactions.

V. ACKNOWLEDGMENTS

The authors extend their sincere appreciation to the Deanship of Scientific Research at King Saud University for its funding this Prolific Research Group (PRG-1436-26).

[1] M. R. Phadatare, A. B. Salunkhe, V. M. Khot, C. I. Sathish, D. S. Dhawale, and S. H. Pawar, J. Alloy Compd. **546**, 314 (2013).
[2] E. Roduner, Chem. Soc. Rev. **35**, 583 (2006).
[3] Z. Zhang, Y. Liu, G. Yao, G. Zu, X. Zhang, and J. Ma, Physica E **45**, 122 (2012).
[4] S. Vivekanandhan, M. Venkateswarlu, D. Carnahan, M. Misra, A. K. Mohanty, and N. Satyanarayana, Ceram. Int. **39**, 4105 (2013).
[5] P. Sivakumar, R. Ramesh, A. Ramanand, S. Ponnusamy, and C. Muthamizhchelvan, Mater. Lett. **66**, 314 (2012).
[6] M. A. Gabal, J. Phys. Chem. Solid **64**, 1375 (2003).
[7] N. Kasapoglu, A. Baykal, Y. Koseoglub, and M. S. Toprak, Scripta Mater. **57**, 441 (2007).
[8] M. A. Gabal, S. Kosa, and T. S. El Muttairi, Ceram. Int. **40**, 675 (2014).
[9] Z. Jia, K. Peng, and L. Xu, Mater. Chem. Phys. **136**, 512 (2012).
[10] S. L. Darshane, S. S. Suryavanshi, and I. S. Mulla, Ceram. Int. **35**, 1793 (2009).
[11] E. Karaoglu, U. Ozel, C. Caner, A. Baykal, M. M. Summak, and H. Sozeri, Mater. Res. Bull. **47**, 4316 (2012).
[12] Y. L. Liu, H. Wang, Y. Yang, Z. M. Liu, H. F. Yang, G. L. Shen, and R. Q. Yu, Sensor Actuat B **102**, 148 (2004).
[13] P. Sivakumar, R. Ramesh, A. Ramanand, S. Ponnusamy, and C. Muthamizhchelvan, J. Alloy Compd. **537**, 203 (2012).
[14] M. Yehia, S. Labib, and S. M. Ismail, Physica B **446**, 49 (2014).
[15] B. D. Cullity, *Elements of X-ray Diffraction*, 2nd Edn., Addison-Wesley Publishing Company, Inc., 324 (1978).
[16] M. Kooti and A. N. Sedeh, J. Mater. Sci. Technol. **29**, 34 (2013).
[17] P. Weiss and R. Forrer, Annalen der Physik **12**, 279 (1929).

DOI:10.1063/1674-0068/29/cjcp1507158